

FICTITIOUS DOMAIN SIMULATIONS FOR THE TWO-PHASE FLOW ENERGY BALANCE OF THE CLOTAIRE STEAM GENERATOR MOCK-UP

Michel Belliard and Isabelle Ramière¹

CEA-Cadarache

DEN/DER/SSTH/LMDL, 13108 St-Paul-Lez-Durance, France

michel.belliard@cea.fr

ABSTRACT

The context of this paper is the numerical simulation of a nuclear component, in the framework of the NEPTUNE platform, by a fictitious domain method. We consider industrial simulations of two-phase flows with the homogeneous equilibrium (or relaxed) model. The introduction of no remeshing fictitious domain method is mainly motivated by free surface studies, fluid-structure interactions or fast Cartesian mesh solvers. As a first step toward a full fictitious domain simulation, this paper focuses on the fictitious domain computation of the energy balance equation of a nuclear component. Considering the steam generator, this equation is solved by a finite-element volume-penalization method. We recall the model used for the energy balance equation and review the modelizations and the computations. An industrial simulation of the steam generator mock-up CLOTAIRE is presented in order to appreciate the accuracy and the limits of the fictitious domain approach. Exploring L_2 -norm error along some vertical enthalpy profiles, we claim that the relative error introduced by the fictitious domain method is globally decreasing with the space step and can be lower than 10^{-3} for space steps around the U-tube diameter size. We conclude that we can reach an enough precision for the industrial applications and benefit from numerical advantages due to the use of Cartesian meshes.

KEYWORDS

Fictitious Domain, NEPTUNE Project, Nuclear Component, Steam Generator, Finite Elements

1 INTRODUCTION

This paper is devoted to industrial numerical simulations of nuclear components: core and steam generator (SG) by a Fictitious Domain Method (FDM) [1, 2]. We consider industrial simulations of two-phase flows with a homogeneous equilibrium or relaxed model (HEM or HRM) [3]. This paper focuses on a particular implementation of a FDM following the works previously realized by Ramière *et al.* [4, 5] in the NEPTUNE platform [6]. This platform is dedicated to the thermal-hydraulics numerical

¹Today at the CEA Valrhô-Marcoule, DEN/DRCP/SCPS/LCSE, BP 17171, 30207 Bagnols sur Cèze, France

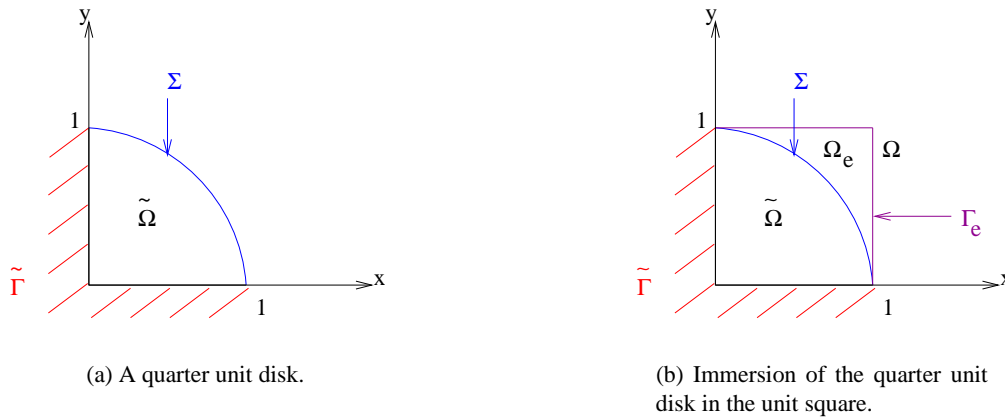


Figure 1: Physical Domain and Fictitious Domain.

simulation of nuclear power plants from the local scale to the system scale through the component scale. As a first step toward a full fictitious domain simulation, the fictitious domain computation of the energy balance equation of a nuclear component is considered. For the steam generator, this equation is solved with the NEPTUNE/pyGene code (3D Q_0/Q_1 finite element method) [7].

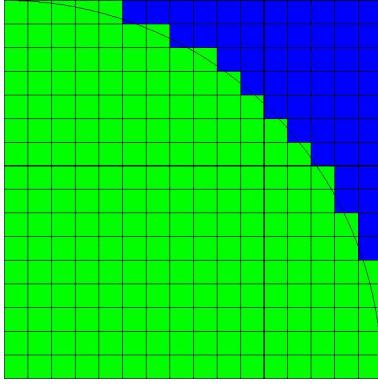
In a fictitious domain context, the physical domain $\tilde{\Omega}$ - see Fig. 1(a) - is immersed into a fictitious domain Ω geometrically bigger and simpler than the physical one - see Fig. 1(b) -. As the fictitious domain geometry is simpler than the physical domain's one, structured (Cartesian) meshes can be used. Doing this, some immersed boundary Σ appears. From the original partial differential equation (PDE) to solve on the physical domain, a new PDE is built on the fictitious domain. The terms of the fictitious problem are designed to handle the immersed BC of the original problem. The new equation is then solved on the fictitious domain without modifying the numerical scheme and without using local unknowns.

Among the advantages of this approach, we are motivated by the use of fast linear solvers for Cartesian mesh, the use of a unique formalism for free, porous or blind, fixed or moving regions without remeshing [8] and the computations of fluid-structure interactions or free-surface flows. Multi-resolution techniques naturally applied within Cartesian mesh is another motivation [9].

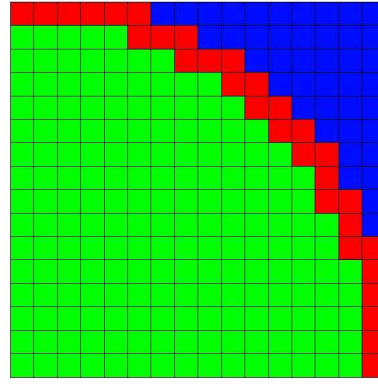
The paper is built as follows. We briefly introduce the fictitious domain methods in Section 2 and the steam generator HEM energy balance equation in Section 3. The application of our FDM to this SG convection-diffusion equation is the object of Section 4. Finally, in order to appreciate the accuracy and the limits of this approach, we present an industrial fictitious domain simulation of the CEA SG mock-up CLOTAIRE in Section 5 and we conclude by a few remarks.

2 A FICTITIOUS DOMAIN METHOD INTRODUCTION

In the papers [10, 11] various fictitious domain methods are presented and tested. In particular, we can modelize the immersed boundary as a thin interface or a spread interface $(\omega_{h,\Sigma})$, see Fig. 2(b) and 2(a). Here, in the FE framework, we only consider the spread interface model, but other choices are discussed in [11] for the interface model with finite volume (FV) method. For instance, we can consider



(a) Thin interface model: $\tilde{\Omega}_h$ and $\Omega_{e,h}$.



(b) Spread interface model: $\tilde{\Omega}_h$, $\omega_{h,\Sigma}$ and $\Omega_{e,h}$.

Figure 2: Partitions of the Fictitious Domain Ω .

the following original convection-diffusion problem in the conservative form. For $\tilde{\mathbf{a}} \in (L^\infty(\tilde{\Omega}))^{d \times d}$, $\tilde{\mathbf{v}} \in (L^\infty(\tilde{\Omega}))^d$, $\tilde{b} \in L^\infty(\tilde{\Omega})$ and $\tilde{f} \in L^2(\tilde{\Omega})$, find $\tilde{u} \in H^1(\tilde{\Omega})$ such that:

$$\begin{cases} -\operatorname{div}(\tilde{\mathbf{a}} \cdot \nabla \tilde{u}) + \operatorname{div}(\tilde{\mathbf{v}} \tilde{u}) + \tilde{b} \tilde{u} = \tilde{f} & \text{in } \tilde{\Omega} \\ \text{B.C.} & \text{on } \partial \tilde{\Omega} \end{cases} \quad (1)$$

The tensor of diffusion $\tilde{\mathbf{a}} \equiv (\tilde{a}_{ij})_{1 \leq i, j \leq d}$ and the reaction coefficient \tilde{b} verify the classical ellipticity assumption (\tilde{u} exists and is unique).

In the \mathcal{Q}_1 finite element (FE) framework, the convection-diffusion fictitious domain problem stands as follow. Find $u_h \in V_h(\Omega) = \{v_h \in C^0(\bar{\Omega}), v_h|_K \in \mathcal{Q}_1 \forall K \in \mathcal{T}_h\} \subset H^1(\Omega)$ such that:

$$\begin{cases} -\operatorname{div}(\mathbf{a} \cdot \nabla u_h) + \operatorname{div}(\mathbf{v} u_h) + b u_h = f & \text{in } \Omega_h \\ \text{physical B.C. for } u_h & \text{on } \partial \Omega_h \cap \partial \tilde{\Omega}_h \\ \text{suitable B.C. for } u_h & \text{on } \partial \Omega_h \setminus \partial \tilde{\Omega}_h \end{cases} \quad (2)$$

where $\mathbf{a} \in (L^\infty(\Omega_h))^{d^2}$, $\mathbf{v} \in (L^\infty(\Omega_h))^d$, $f \in L^2(\Omega_h)$ and $b \in (L^\infty(\Omega_h))$ such that \mathbf{a} , b verify the classical ellipticity assumption in Ω_h (u_h exists and is unique).

The terms b and f enable to take Dirichlet ($\tilde{u} = u_R$), Neumann ($-(\tilde{\mathbf{a}} \cdot \nabla \tilde{u}) \cdot \mathbf{n} = g_R$) or Robin BC ($-(\tilde{\mathbf{a}} \cdot \nabla \tilde{u}) \cdot \mathbf{n} = \alpha_R(\tilde{u} - u_R) + g_R$) into account on the immersed boundary Σ where \mathbf{n} is the outward normal unit vector. We focus here on the Robin BC formalism because Dirichlet BC can be deduced of the Robin BC expression by penalization techniques.

From the analysis of a continuous transmission problem between the physical region $\tilde{\Omega}$ and the external one $\Omega_e = \Omega \setminus \tilde{\Omega}$, equipped with zero diffusion and convection fluxes, a flux-jump term naturally appears across Σ [10]. This surface integral of the jump of fluxes is changed into a volume integral on the spread

interface $\omega_{h,\Sigma}$:

$$\int_{\Sigma} \{ \alpha_R (\tilde{u} - u_R) + g_R + (\tilde{\mathbf{v}} \cdot \mathbf{n}) \tilde{u} \} ds = \int_{\omega_{h,\Sigma}} (\alpha_R (u_h - u_R) + g_R + (\mathbf{v} \cdot \mathbf{n}) u_h) \frac{dx}{\epsilon_h} \quad (3)$$

where ϵ_h is a ad-hoc coefficient to ensure this equality [10]. For sake of simplicity, we denote ϵ_h by ϵ in the rest of the paper. Then, the coefficients of the fictitious domain problem (2) are defined as follow. Let $0 < \eta < \epsilon < 1$ be a real penalty parameter which is likely to tend to zero, we set for the discrete physical region $\tilde{\Omega}_h$

$$\mathbf{a}|_{\tilde{\Omega}_h} = \tilde{\mathbf{a}}|_{\tilde{\Omega}_h}, \quad \mathbf{v}|_{\tilde{\Omega}_h} = \tilde{\mathbf{v}}|_{\tilde{\Omega}_h}, \quad b|_{\tilde{\Omega}_h} = \tilde{b}|_{\tilde{\Omega}_h}, \quad f|_{\tilde{\Omega}_h} = \tilde{f}|_{\tilde{\Omega}_h}, \quad (4)$$

for the spread interface $\omega_{h,\Sigma}$

$$\mathbf{a}|_{\omega_{h,\Sigma}} = \tilde{\mathbf{a}}|_{\omega_{h,\Sigma}}, \quad \mathbf{v}|_{\omega_{h,\Sigma}} = \tilde{\mathbf{v}}|_{\omega_{h,\Sigma}}, \quad b|_{\omega_{h,\Sigma}} = \tilde{b}|_{\omega_{h,\Sigma}} + \frac{\alpha_R}{\epsilon} + \frac{\mathbf{v} \cdot \mathbf{n}}{\epsilon}, \quad f|_{\omega_{h,\Sigma}} = \tilde{f}|_{\omega_{h,\Sigma}} + \frac{\alpha_R u_R - g_R}{\epsilon}, \quad (5)$$

and for the discrete external region $\Omega_{e,h}$

$$\mathbf{a}|_{\Omega_{e,h}} = \eta \mathbf{Id}, \quad \mathbf{v}|_{\Omega_{e,h}} = \mathbf{0}, \quad b|_{\Omega_{e,h}} = 0, \quad f|_{\Omega_{e,h}} = 0. \quad (6)$$

Choosing $\frac{\alpha_R}{\epsilon} = \frac{1}{\eta}$ and $\frac{g_R}{\epsilon} = 0$, we can imposed Dirichlet BC ($\tilde{u} = u_R$) by spread interface L^2 penalization. Then, $b|_{\omega_{h,\Sigma}} \approx \frac{1}{\eta}$ and $f|_{\omega_{h,\Sigma}} \approx \frac{u_R}{\eta}$ (we have assume that the others coefficients are negligible compared to $\frac{1}{\eta}$).

Moreover, a quick glance at a naive extension of this scheme to the Navier-Stokes equation indicates that the choice $\frac{\alpha_R}{\epsilon} \propto \frac{1}{K}$, $\frac{\alpha_R u_R}{\epsilon} = 0$ and $\frac{g_R}{\epsilon} = 0$ can provide a unified description of free ($K \rightarrow +\infty$), porous (K : a physical permeability value) or blind regions ($K = \eta \rightarrow 0$) [8]. Let us notice that it is already a natural way to deal with the tube bundle (porous regions) and the free flow regions in the context of the homogenization techniques used for the nuclear component simulation [7].

Using a $\mathcal{O}(h^2)$ FE scheme, Ramière *et al.* have shown that this fictitious domain approach leads to $\mathcal{O}(h)$ results (due to the approximate position of the boundary in the Cartesian mesh) [10]. In order to improve the accuracy of the solution (but not the order of convergence), Adaptive Mesh Refinement (AMR) techniques are necessary, as the Local Defect Correction method [12] or the FIC-EBC method for a FV space discretization [11].

3 STEAM GENERATOR HEM ENERGY BALANCE EQUATION

In the NEPTUNE/pyGene code, the two-phase secondary fluid is modeled by an equivalent mixture fluid through a homogenization process [7]. The HEM approach leads to three balance equations: mass, momentum and energy. Momentum and energy disequilibrium can be taken into account through physical models. We are interested in the stationary regime, obtained with a march in time algorithm. The secondary fluid energy balance equation is a convection-diffusion like equation, in a non-conservative

form (which can be transformed in a conservative equation using the mass balance equation), with non-linear source terms. The unknown is the specific enthalpy H ($KJ.kg^{-1}$). For our application concerning the energy balance equation only, the mixture pressure P (Pa) and mass flow \mathbf{G} ($\equiv \rho\mathbf{V}$, with \mathbf{V} the mixture velocity ($m.s^{-1}$)), are considered as data (previously computed values).

$$\beta\rho\partial_t H + \beta\mathbf{G}.\nabla H - \text{div}(\beta\chi_T\nabla H) = \beta Q - \text{div}(\beta x(1-x)\rho\mathcal{L}\mathbf{V}_R), \quad (7)$$

where

- β is the porosity ($\equiv \omega_m/\omega$) with ω the homogenization cell volume (m^3) and ω_m the mixture volume (liquid + steam) in the homogenization cell (m^3),
- $\rho(H, P)$ is the density ($kg.m^{-3}$),
- $\chi_T = a|\mathbf{G}|L$ is the turbulent diffusion coefficient ($kg.m^{-1}.s^{-1}$) with a the Schlichting's coefficient, L a typical eddy length and $|\cdot|$ the Euclidean norm [13],
- Q is the heat source term ($W.m^{-3}$),
- \mathbf{V}_R is the relative velocity (steam velocity minus liquid velocity, $m.s^{-1}$) [14, 15],
- $x(H, P)$ is the static quality ($\equiv \frac{H - H_{ls}}{\mathcal{L}}$) with $H_{ls}(P)$ the saturation liquid enthalpy ($KJ.kg^{-1}$) and $\mathcal{L}(P)$ the latent heat ($J.kg^{-1}$).

The $\beta x(1-x)\rho\mathcal{L}\mathbf{V}_R$ term is called the drift term. The heat source term Q is given by the resolution of the primary fluid balance equation in which external correlations, involving H et \mathbf{G} , are used.

In the NEPTUNE/pyGene code, the space discretization of the weak form of the Equation (7) is done by \mathcal{Q}_1 finite elements (H , \mathbf{V} and β) and \mathcal{Q}_0 finite elements (P , ρ , \mathbf{G} , χ_T and Q). The drift term is approximated using \mathcal{Q}_1 finite elements. Balancing Tensor Diffusivity correction [16] is applied to prevent spurious oscillations introduced by the central difference discretization of the convection term. The time discretization is done by the Crank-Nicholson method. The RHS of Equation (7) are explicited. The stationary flow regime is obtained when

$$\frac{\|H^{n+1} - H^n\|_{L^2}}{\|H^n\|_{L^2}\Delta t} \leq 10^{-5} s^{-1}, \quad (8)$$

where the time step Δt is restricted by a CFL condition with a coefficient of 2.5. At each time step, linear systems are smoothed by 20 ILLU preconditioned CGS iterations [17]. Iterations are early stopped if the initial residual is reduced by a 10^7 factor.

4 A FE FICTITIOUS DOMAIN FORMULATION OF THE ENERGY BALANCE EQUATION

In the FE context, the fictitious domain formulation of the Equation (7) on the spread interface $\omega_{h,\Sigma}$ writes as ($\omega_e \in \omega_{h,\Sigma}$):

$$\begin{aligned} & \sum_e \rho_e \int_{\omega_e} \xi^i \beta \partial_t H + \sum_e \mathbf{G}_e \cdot \int_{\omega_e} \xi^i \beta \nabla H \\ & + \sum_e \chi_{T_e} \int_{\omega_e} \beta \nabla H \cdot \nabla \xi^i - \sum_e \chi_{T_e} \int_{\partial \omega_e \cap \partial \Omega_h} \xi^i \beta \nabla H \cdot \mathbf{n} + \mathcal{A}(H) \\ & = \sum_e Q_e \int_{\omega_e} \xi^i \beta - \sum_e \int_{\omega_e} \xi^i \operatorname{div}(\beta x(1-x)\rho L \mathbf{V}_R) + \mathcal{B}(H_D) \end{aligned} \quad (9)$$

where ξ^i are the Q_1 FE basis functions and \mathbf{n} the external normal. The extra-terms \mathcal{A} and \mathcal{B} are the FE additional parts of the terms b and f of Equation (2), described in (5), depending on α_R , u_R and g_R . Let's notice that the term $\mathbf{v} \cdot \mathbf{n}$ of Equation (5) is here equal to $\frac{\mathbf{G} \cdot \mathbf{n}}{\rho}$. Usually the steam generator energy balance equation is equipped with Dirichlet (inflow regions) and homogeneous Neumann (outflow regions and walls) boundary conditions.

For a Dirichlet boundary condition ($H = H_D$), these terms are given by the penalization of the spread interface nodes. Using Equations (5) with $\alpha_D := \frac{\alpha_R}{\epsilon} = \frac{1}{\eta}$, $u_R = H_D$, $\frac{\mathbf{v} \cdot \mathbf{n}}{\epsilon} \ll \frac{1}{\eta}$ and $\frac{g_R}{\epsilon} = 0$, we get:

$$\mathcal{A}(H) = \sum_e (\alpha_D)_e \sum_j H_j \int_{\omega_e} \xi^i \xi^j \quad (10)$$

$$\mathcal{B}(H_D) = \sum_e (\alpha_D)_e (H_D)_e \int_{\omega_e} \xi^i \quad (11)$$

For a Neumann boundary condition ($-\chi_{T_e} \beta \nabla H \cdot \mathbf{n} = g_N$) on the walls ($\mathbf{V} \cdot \mathbf{n} = 0$), the same equations with $\frac{\alpha_R}{\epsilon} = 0$, $\frac{\mathbf{v} \cdot \mathbf{n}}{\epsilon} = 0$ and $g_R = g_N$, we get:

$$\mathcal{B}(g_N) = \sum_e \frac{(g_N)_e}{\epsilon_e} \int_{\omega_e} \xi^i \quad (12)$$

In case of homogeneous Neumann boundary condition ($g_N = 0$), this term is null.

5 THE FICTITIOUS DOMAIN CLOTAIRE MOCK-UP SIMULATION

Academic test cases involving analytic solutions, extensively studied in [10] and [11], illustrate the numerical method convergence. Elements concerning CPU time performance comparison are also given in [11]. In this paper, we focus exclusively on the capability of the method to deal with an industrial problem without any known analytic solution. The emphasis is on the accuracy and on the limits of this approach.

CLOTAIRE [18] is dedicated to the qualification of the steam generator 3D simulation codes. This mock-up has the real scale in elevation of an AREVA-NP SG. Fig. 3 shows a 2D CLOTAIRE's scheme. The

mock-up's geometry is approximately 9.17 m height (z coordinate) and 0.62 m diameter half-cylinder (x and y coordinates). The liquid secondary fluid comes into the riser by an approximately 0.1 m height half-cylindrical window and is heated by the hot primary fluid circulating in the U-tubes. A liquid/steam mixture is then obtained. In real SGs and after liquid separation, the steam turns on the turbines. We distinguish the so-called hot leg (primary fluid inlet) and the cold leg (primary fluid outlet).

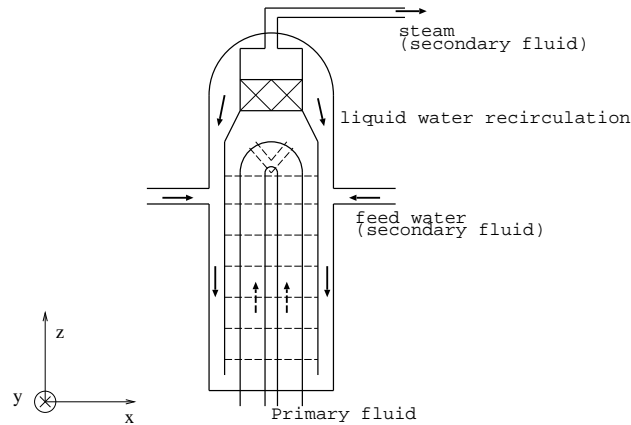


Figure 3: CLOTAIRE Mock-up Scheme.

We don't have any analytic solution for this problem, hence we consider a 143,360-cell adapted-mesh approximation as reference solution (it is the maximum number of cells for solving all the flow balance equations on a standard personal computer). The mean radial space step $h_x = h_y = 1.1 \cdot 10^{-2}$ m is around the distance between the primary fluid U-tubes but the aspect ratio (vertical ratio) is around 7.5 ($h_z = 8.2 \cdot 10^{-2}$ m). This unstructured mesh is very non-uniform in order to be body-fitted to the physical domain and the inner structures (U-tube support plates).

The half-cylinder of the physical domain is immersed into a rectangular parallelepiped chosen as the fictitious domain (see. Fig. 4(a) and 4(b)). Three Cartesian meshes involving 7,200, 57,600 and 460,800 cells are used. The space step is divided by two in each direction from one mesh to the other. For the 460,800-cell mesh, space steps ($h_x = 1.3 \cdot 10^{-2}$ m, $h_y = 1.4 \cdot 10^{-2}$ m and $h_z = 2.3 \cdot 10^{-2}$ m) are close to the reference simulation ones (but the aspect ratio is around 2).

The mixture mass flow \mathbf{G} and pressure P fields are interpolated from this reference solution by a cell nodes trilinear interpolation and a cell barycenters canonic injection respectively. We set $P = \bar{P}$ and $\mathbf{G} = \mathbf{0}$ in the external domain cells ($\Omega_{e,h}$), where \bar{P} denotes the mean pressure. For the nodes and the barycenters of the spread boundary cells ($\omega_{h,\Sigma}$) lying outside the physical domain $\tilde{\Omega}$, we extend the inner domain values by an average process. Fig. 4(c) shows the interpolated mass fluxes at the top of the computation domain (outflow).

Using the same FE code², we would compare fictitious domain computations to the classical ones involving physical domain body-fitted meshes (where H , P and \mathbf{G} are computed together). To prove the capability of the method in industrial simulations, we focus our attention on the accuracy of the fictitious

²We use the same set of constitutive relations which are independent of the numerical method used.

domain computations (no CPU consideration is made).

5.1 The Simulation Conditions

The energy balance equation boundary conditions are:

- Dirichlet: inflow hot leg enthalpy $H = 119.3 \text{ KJ.kg}^{-1}$, inflow cold leg enthalpy $H = 118.5 \text{ KJ.kg}^{-1}$,
- Homogeneous Neumann: zero enthalpy flux elsewhere.

The initial condition for the enthalpy is given by a linear profile from 118.5 KJ.kg^{-1} on the U-tube plate to 140 KJ.kg^{-1} at outflow.

5.2 The Immersed Boundary and the Fictitious Domain Boundary

The approximate immersed boundary is analytically computed. For each cell crossed by the immersed boundary, we have the elementary boundary measure S_e , the boundary barycenter \mathbf{x}_e and the physical domain volume ratio r_{ϕ_e} . About 15% of the cells are located outside the physical domain. The external domain is considered as an obstacle for the fluid and the porosity for the element $e \in \Omega_{e,h}$ is reduced by $(1 - r_{\phi_e})$.

We add fictitious domain terms (10) and (11) in Equation (9). The spread boundary elements $e \in \omega_{h,\Sigma}$ located into the half-cylindrical inflow window are volume L^2 penalized (Dirichlet): $(\alpha_D)_e = \frac{1}{\eta}$ with $\eta = 10^{-5}$ and $(H_D)_e = 119.3 \text{ KJ.kg}^{-1}$ or 118.5 KJ.kg^{-1} according to the element position (hot or the cold leg), cf Fig. 5. Simulations have been done with $\eta = 10^{-9}$ leading to similar results but with a worse preconditioned matrix. Nothing has to be done on the spread interface elements located into the half-cylindrical wall as a homogeneous Neumann ($g_N = 0$) BC has to be imposed.

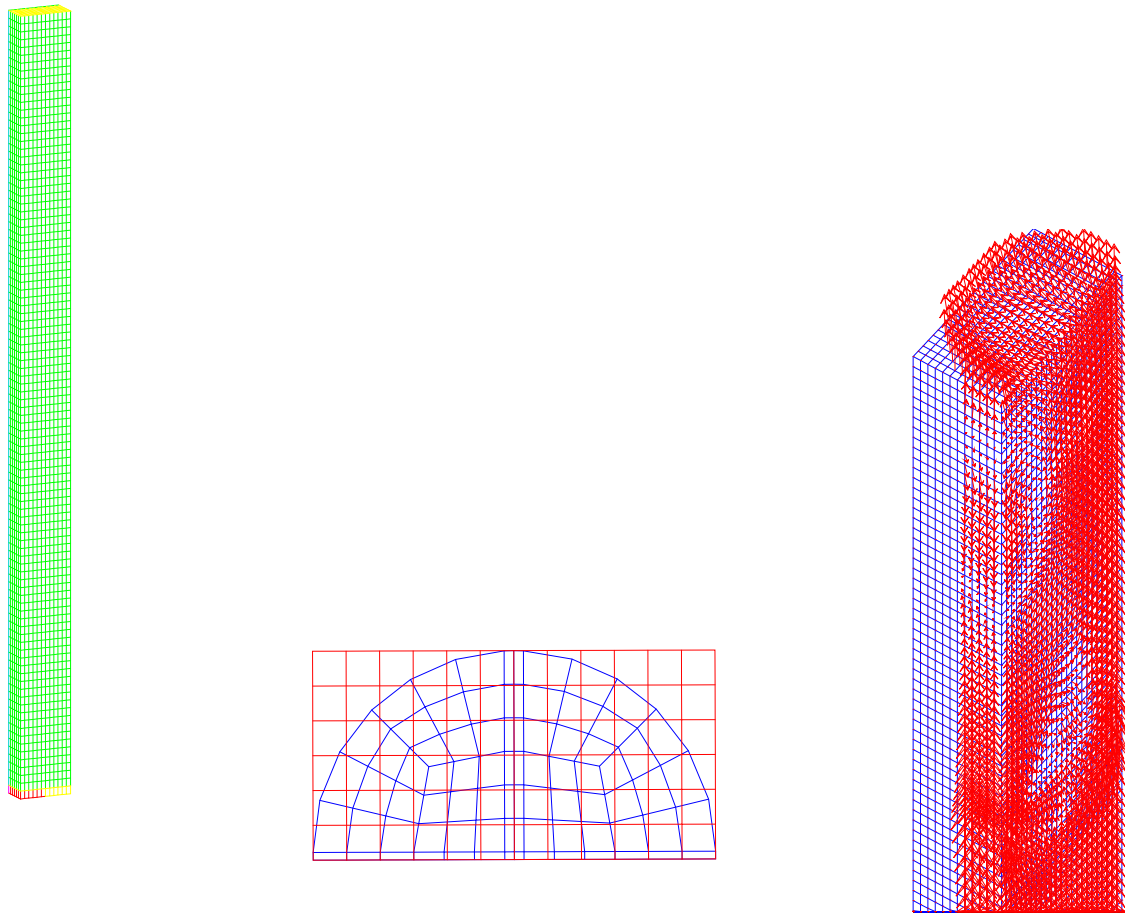
Concerning the fictitious domain boundary itself $\partial\tilde{\Omega}_h$, we impose mixed boundary conditions: homogeneous Neumann BC everywhere except on the external faces in front of the immersed boundary Dirichlet elements ($\omega_{h,\Sigma}$ volume L^2 penalized) and without any intersection with the physical domain boundary $\partial\tilde{\Omega}_h$. On these particular faces, we impose the values of the correspondent Dirichlet immersed boundary conditions (see Fig. 4(a), red and yellow).

5.3 Results

Results can be appreciated through criteria concerning some physical quantities as the global primary/secondary fluid heat exchange, the enthalpy distribution, the enthalpy z -profiles and the relative L^2 -norm error (calculated from the reference solution).

The stationary regime is reached after 441, 1,080 and 2,719 time steps for the 7,200, 57,600 and 460,800-cell meshes respectively. This is similar to the number of time steps required in the case of adapted grids with similar minimum space steps.

The global primary/secondary fluid heat exchange is recovered with a relative error from 10^{-3} (7,200-cell mesh) to 10^{-4} (57,600-cell mesh) in comparison to the reference computation. Fig. 6 shows H isovalues for a horizontal cut plane at half elevation. Reference solution (top) is compared to the fictitious domain solution obtained with the 57,600-cell mesh (bottom). Qualitatively the results are very close (even



(a) Fictitious domain mesh.

(b) Physical domain adapted mesh (blue) and fictitious Cartesian mesh (red) - horizontal cut plane-

(c) Mixture mass flow field for the fictitious domain computation.

Figure 4: Physical Domain and Cartesian Fictitious Domain Meshes. Example of Interpolated Data in the Fictitious Domain.

if we can see some little discrepancies due to the cell-number difference³) and the isovalue lines are perpendicular to the wall (as expected for a homogeneous Neumann boundary condition).

Examples of trilinear interpolations for the enthalpy profiles at a position $x = +/- 0.2$ m and $y = 0.14$ m (denoted c3) are drawn in Fig. 7(a) where Cartesian mesh approximations are compared to the reference solution. The Cartesian mesh profiles are very close to the reference solution ones. Moreover, the finer is the Cartesian mesh, the closer is the approximation: the fictitious domain solutions converge with the mesh step. The relative discrete L^2 -norm error, computed by difference with the reference solution,

³The reference solution is more accurate since it involves a larger number of cells in the physical domain.

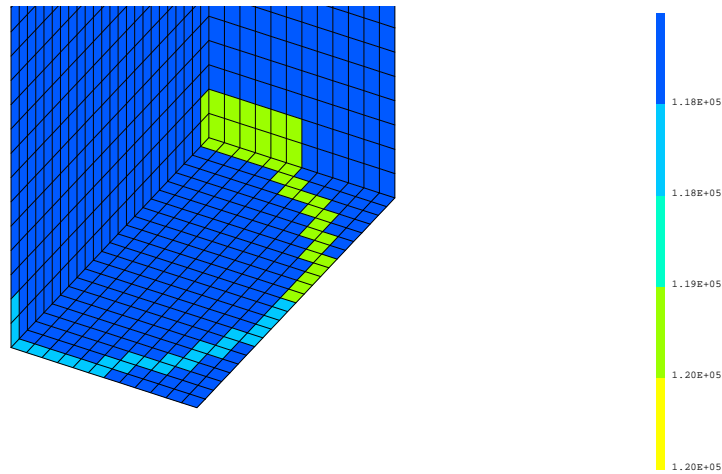


Figure 5: Dirichlet Values H_{D_e} Imposed by Volume L^2 Penalization on Immersed Boundary Element (detail).

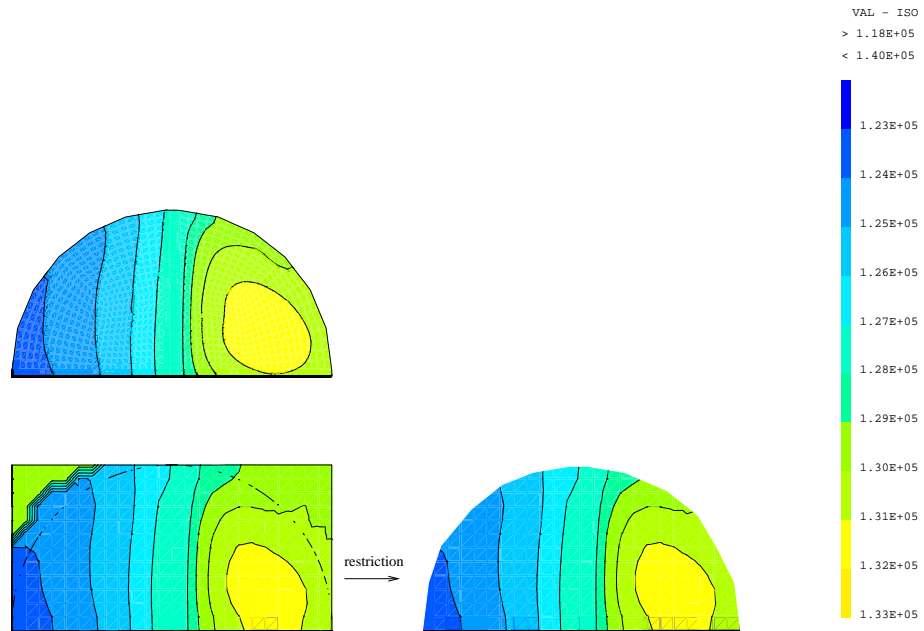
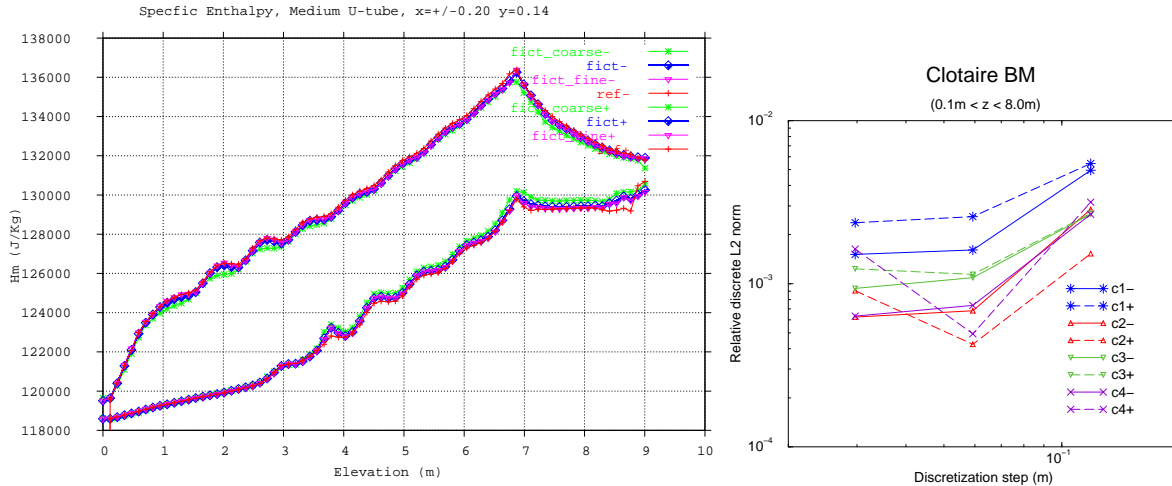


Figure 6: Enthalpy Isovalues for a Horizontal Cut Plane at 5 m (half elevation). Adapted-mesh reference solution (top) and 57,600-cell Cartesian mesh (bottom).



(a) Medium U-tube (c3) specific enthalpy profiles.

(b) Relative L^2 -norm error versus the cell diagonal size ($0 \leq z \leq 8$ m).

Figure 7: Specific Enthalpy Profiles and Relative L^2 -norm Error. Cartesian approximations for meshes with 7,200 (fict_coarse), 57,600 (fict) and 460,800 (fict_fine) cells and reference solution (ref). The notation '+' (respectively '-') is related to the hot leg (respectively the cold leg).

is shown in Fig. 7(b). As a whole, the error decreases with the space step and is always lower than $5 \cdot 10^{-3}$. The fictitious domain solution converges toward the approximate reference solution. However, a quasi-minimum error value is reached for a space step around $5 \cdot 10^{-2}$ m (57,600-cell mesh) and doesn't significantly decrease for lower space steps. Maybe the solution associated to the fictitious domain method using a uniform Cartesian mesh and low aspect ratio cells is nearer from the real solution of the equation than the solution obtained with the classical body-fitted method using an very non-uniform unstructured mesh and high aspect ratio cells.

This simulation illustrates the good properties of this fictitious domain method. Moreover, this method can be easily introduced in an pre-existing industrial code and leads to a enough precision for the industrial application.

6 CONCLUSIONS

In this paper, we have presented the first numerical resolution of the energy balance equation for a nuclear component (here, a steam generator) by a fictitious domain method. The two-phase flow model used is the homogeneous equilibrium model in the framework of the finite element method (3D Q_0/Q_1 elements). It is a first step toward a full fictitious domain simulation involving all the balance equations. The convection-diffusion equation with source terms is solved by a fictitious domain method in a domain with a geometry simpler than the physical domain's one (a rectangular parallelepiped instead of a half-cylinder). A Cartesian mesh can then be used of the classical body-fitted mesh. The immersed interface is

approximated by a spread interface. The immersed Dirichlet BC is enforced by a volume L^2 penalization of the spread interface and the immersed Robin/Neumann BC is imposed by transformation of the flux surface integral into a volume source term located on the spread interface.

An industrial simulation of the steam generator mock-up CLOTAIRE is driven in order to appreciate the accuracy and the limits of this approach in comparison to classical body-fitted mesh methods usually employed in industrial simulations. As a whole, observing physical criteria as the global primary/secondary fluid heat exchange, enthalpy distributions or $L2$ -norm errors, the accuracy of the fictitious domain method is demonstrated. We claim that the relative error introduced by the fictitious domain method globally decreases with the space step and can be lower than 10^{-3} for space steps around the U-tube diameter size. The reached precision is enough for industrial applications and the use of Cartesian meshes is full of promise.

The fictitious domain approach can be obviously used with other space discretization methods as the finite volume method [11]. In this case, the thin interface model is preferred. Academic numerical tests have shown good results in terms of algorithm convergence and accuracy. A further closely related project will be the simulation of the same SG mock-up CLOTAIRE with a fictitious domain VF method. Another planned task is the extension of our fictitious domain method to the computation of the full balance equations.

ACKNOWLEDGMENTS

This work has been achieved in the frame of the NEPTUNE project and financially supported by CEA, EDF, IRSN and AREVA-NP.

References

- [1] V. K. Saul'ev, "On the solution of some boundary value problems on high performance computers by fictitious domain method," *Siberian Math. Journal*, Vol. **4**, No. 4, pp. 912–925, (1963) [in Russian].
- [2] G.I. Marchuk, *Methods of Numerical Mathematics*, Springer-Verlag, New York, USA, 1982 (1rst ed. 1975).
- [3] S. Clerc, "Numerical simulation of the Homogeneous Equilibrium Model for Two-phase Flows." *Journal of Computational Physics*, Vol. **161**, No. 1, pp. 354–375, 2000.
- [4] I. Ramière, Ph. Angot, and M. Belliard, "Fictitious domain methods to solve convection-diffusion problems with general boundary conditions," *Proc. in the 17th Computational Fluid Dynamics Conference AIAA*, Toronto, Canada, June (2005).
- [5] I. Ramière, Ph. Angot, and M. Belliard, "On the simulation of Nuclear Power Plant Components using a fictitious domain approach," *Proc. in the 11th International Topical Meeting on Nuclear Thermal-Hydraulics (NURETH-11)*, Avignon, France, October 2-6 (2005).
- [6] A. Guelfi and *al.*, "A new multi-scale platform for advanced nuclear thermal-hydraulics status and prospects of the NEPTUNE project," *11 th International Topical Meeting on Nuclear Reactor Thermal-Hydraulics (NURETH-11)*, Avignon, France, October 2-6 (2005).

- [7] M. Grandotto and P. Obry, “Calculs des écoulements diphasiques dans les échangeurs par une méthode aux éléments finis,” *Revue Européenne des Eléments Finis*, Vol. **5**, No. 1, pp. 53–74, (1996) [in French].
- [8] K. Khadra, Ph. Angot, S. Parneix, and J.P. Caltagirone, “Fictitious Domain Approach for Numerical Modelling of Navier-Stokes Equations.” *International Journal for Numerical Methods in Fluids*, Vol. **34**, No. 8, pp. 651–684, 2000.
- [9] O. Roussel and K. Schneider, “An adaptive multiresolution method for combustion problems : Application to flame ball-vortex interaction,” *Computers and Fluids*, Vol. **34**, pp. 817–831, 2005.
- [10] I. Ramière, Ph. Angot, and M. Belliard, “A fictitious domain approach with spread interface for elliptic problems with general boundary conditions,” *Computer Methods in Applied Mechanics and Engineering*, Vol. **196**, No. 4-6, pp. 766–781, (2007).
- [11] I. Ramière, Ph. Angot, and M. Belliard, “A general fictitious domain method with immersed jumps and non-conforming structured mesh,” *Journal of Computational Physics*, Vol. **225**, No. 2, pp. 1347–1387, (2007).
- [12] W. Hackbusch, *Local Defect Correction Method and Domain Decomposition Techniques*, Vol. 5 of *Computing Suppl.*, Springer-Verlag, Wien, (1984).
- [13] H. Schlichting, *Boundary Layer Theory*, Mac Graw Hill, New York, USA, (1968).
- [14] N. Zuber and J.A. Findlay, “Average Volumetric Concentration in Two-Phase Flow Systems,” *J. Heat Transfert*, Vol. **87**, No. 4, pp. 453–468, (1965).
- [15] G. S. Lellouche and B. A. Zolotar, “Mechanistic Model For Predicting Two-Phase Void Fraction For Water in Vertical Tubes, Channels, and Rod Bundles,” Tech. rep., EPRI, (1982).
- [16] P.M. Gresho, S.T. Chan, R. L. Lee, and C.D Upson, “A modified Finite Element Method for Solving the Time-Dependent Incompressible Navier Stokes Equations (Part 1: Theory),” *Int. J. Num. Methods in Fluids*, Vol. **4**, No. 6, pp. 557–598, (1984).
- [17] H.H. Van Der Vorst, “BI-CGStab and smoothly converging variant of BI-CG for the solution of nonsymmetric linear systems.” *SIAM J. Sci. Statist. Comput.*, Vol. **13**, No. 2, pp. 631–644, (1992).
- [18] J.L. Campan and J.C. Bouchter, “Steam generator experiment for advanced computer code qualification : CLOTAIRE international program,” *Third International Topical Meeting on Nuclear Power Plant Thermohydraulics and Operations*, Seoul, April (1988).